Kybernetika

Zhen Wang; Wei Sun; Zhouchao Wei; Xiaojian Xi

Dynamics analysis and robust modified function projective synchronization of Sprott E system with quadratic perturbation

DYNAMICS ANALYSIS AND ROBUST MODIFIED FUNCTION PROJECTIVE SYNCHRONIZATION OF SPROTT E SYSTEM WITH QUADRATIC PERTURBATION

Zhen Wang, Wei Sun, Zhouchao Wei and Xiaojian Xi

Hopf bifurcation, dynamics at infinity and robust modified function projective synchronization (RMFPS) problem for Sprott E system with quadratic perturbation were studied in this paper. By using the method of projection for center manifold computation, the subcritical and the supercritical Hopf bifurcation were analyzed and obtained. Then, in accordance with the Poincare compactification of polynomial vector field in R^3, the dynamical behaviors at infinity were described completely. Moreover, a RMFPS scheme of this special system was proposed and proved based on Lyapunov direct method. The simulation results demonstrate the correctness of the dynamics analysis and the effectiveness of the proposed synchronization strategy.

Keywords: Hopf bifurcation, center manifold theorem, Poincare compactification, robust modified function projective synchronization, chaotic systems

Classification: 34H10, 34H20, 93C15

1. INTRODUCTION

In the past three decades, many 3D autonomous hyperbolic type chaotic systems have been extensively studied and found ubiquitous applications in science, engineering and mathematical communities [1,16,24]. In these papers, researchers mainly concentrate on three aspects, chaotic system constructing, chaos control and chaos applications. Based on a classification condition formulated by Vaněček and Čelikovský [21], these chaotic systems satisfy $a_{12}a_{21} > 0$, $a_{12}a_{21} < 0$, or $a_{12}a_{21} = 0$. Moreover, according to the classification developed in [26], they are classified into the Lorenz system group if $a_{11}a_{12} < 0$, the Chen system group if $a_{11}a_{12} < 0$, or the Yang–Chen system (transition system) group if $a_{11}a_{12} = 0$. Most of the studied chaotic systems belong to the Shilnikov type, but the Shilnikov criteria is not sufficient-necessary condition for emergence of chaos. So it is very important to generate a new simple chaotic system which doesn't belong to Shilnikov type chaos. In Ref. [19] Sprott considered some ordinary differential equations of chaotic systems with one stable equilibrium but less than seven items and only contain one or two nonlinearities in 1994. In Ref. [22], Wang considered a new chaotic with one stable equilibrium based on Sprott E system by adding a constant

number to the first equation. To investigate the chaos of these systems, in Ref. [25], we consider a generalized chaotic system with one stable equilibrium

$$\dot{x} = yz + h(x), \quad \dot{y} = x^2 - y, \quad \dot{z} = 1 - 4x, \tag{1}$$

where $h(x) = ex^2 + fx + g$. Obviously, it has only one equilibrium $E\left(\frac{1}{4}, \frac{1}{16}, -e - 4f - 16g\right)$. Let $\tilde{x} = x - \frac{1}{4}$, $\tilde{y} = y - \frac{1}{16}$, $\tilde{z} = z + e + 4f + 16g$, then the system (1) can be transformed into

$$\dot{\tilde{x}} = \left(\frac{e}{2} + f\right)\tilde{x} - (e + 4f + 16g)\tilde{y} + \frac{1}{16}\tilde{z} + e\tilde{x}^2 + \tilde{y}\tilde{z}, \dot{\tilde{y}} = \frac{1}{2}\tilde{x} - \tilde{y} + \tilde{x}^2, \dot{\tilde{z}} = -4\tilde{x} \tag{2}$$

which has one equilibrium $O(0,0,0)$. Since this system is different from the existing Shilnikov type chaotic systems, it is important and necessary to further study the dynamics on the basis of the Ref. [25], such as the existence of periodic orbits, the qualitative analysis of infinite points etc.

Furthermore, the generation mechanism of chaos has been an active research topic since Lorenz system was proposed. Generally chaos behavior is understood as a result of interplay between stable manifold and unstable manifold of a unstable equilibrium or some equilibria. Ref. [22] added a simple constant control parameter to Sprott E chaotic system, which can generate chaotic attractors with only one stable equilibrium and reveal some new mysterious features of chaos. Inspired by this idea, we report a simple three-dimensional autonomous chaotic system with only one stable node-focus equilibrium in Ref. [25]. The discovery of this new system is interesting, because with a single stable equilibrium in a 3D autonomous quadratic system, one typically would anticipate non-chaotic behaviors. Yet, this system is chaotic. Therefore, it is necessary to explore whether there are other simple 3D autonomous chaotic systems only with one stable equilibrium and at most six terms including only one or two nonlinear terms such that the topological structure of these systems and the proposed system by Wang and Chen [22] are different?

On the other hand, researchers frequently encounters chaos control and chaos synchronization problems in many physical chaotic systems, and they have developed many methods and techniques over the last few decades, such as feedback approach, adaptive method and different kinds of synchronization: complete synchronization (CS, i.e. Identical synchronization (IS)), phase synchronization (PS), lag synchronization (LS), anticipatory synchronization (AS), GS, multiplexing synchronization (MS) etc. [2, 13, 23]. In recent years, function projective synchronization (FPS) was proposed in Ref. [10]. Furthermore, In Ref. [20] MFPS of two hyperchaotic systems was designed. However, most existing MFPS does not consider the parameters perturbation in realistic systems. It is an ideal candidate for examining RMFPS for the system (1).

Meanwhile, the chaotic attractor of the system (1) with only one stable equilibrium is a hidden attractor which has a basin of attraction that does not intersect with small neighborhoods of any equilibrium points [8, 11–12]. In engineering applications, hidden attractors allow unexpected and potentially disastrous responses to perturbations in a structure like a bridge or an airplane wing. So we can see that the study of the dynamics of the system (1) and RMFPS for this system is of high practical importance. Hopf bifurcation, dynamics at infinity and RMFPS are researched in this paper. The

paper is organized as follows. Hopf bifurcation based on center manifold theorem is presented in Sec. 2. In Sec. 3, dynamical behaviors at infinity are obtained by using the Poincare compatification of polynomial vector field in R^3. Also, RMFPS is designed and proved by using Lyapunov direct method in Sec. 4. In Sec. 5, numerical simulations are provided to illustrate the subcritical and the supercritical Hopf bifurcation together with the performance of the proposed synchronization strategy. Finally, some concluding remarks are presented in the final section.

2. HOPF BIFURCATION ANALYSIS

Rewrite the system (2) as

$$\dot{X} = JX + F(X) \tag{3}$$

where

$$J = \begin{pmatrix} \frac{e}{2} + f & -e - 4f - 16g & \frac{1}{16} \\ \frac{1}{2} & -1 & 0 \\ -4 & 0 & 0 \end{pmatrix}, \ F(X) = \begin{pmatrix} e\tilde{x}^2 + \tilde{y}\tilde{z} \\ \tilde{x}^2 \\ 0 \end{pmatrix}, \ X = (\tilde{x}, \tilde{y}, \tilde{z})^{\mathrm{T}}.$$

Suppose that the function $F(X)$ is represented as $F(X) = \frac{1}{2}A(u,v) + \frac{1}{6}B(u,v,w)$ $+ O(\|X\|^4)$, and $A(u,v)$, $B(u,v,w)$ are symmetric multilinear vector functions,

$$A(u,v) = \begin{pmatrix} 2eu_1v_1 + u_2v_3 + u_3v_2 \\ 2u_1v_1 \\ 0 \end{pmatrix}, \quad B(u,v,w) \equiv 0.$$

Theorem 2.1. The Hopf bifurcation of system (1) on the bifurcation surface on $1 - f - \frac{e}{2} > 0$, $\frac{1}{4} + f + 8g > 0$, and $\frac{e}{2} - 8g \leq \frac{1}{4}$.

P r o o f.   Obviously, the characteristic polynomial is

$$f(\lambda) = \lambda^3 + \left(1 - f - \frac{e}{2}\right)\lambda^2 + \left(\frac{1}{4} + f + 8g\right)\lambda + \frac{1}{4}.$$

Suppose $f(\lambda)$ has a pair of pure imaginary roots $\lambda_{1,2} = \pm i\omega$ and a negative root λ_3 and substitute these into $f(\lambda)$, it then follows that

$$\lambda_3 = -\left(1 - f - \frac{e}{2}\right) < 0, \omega^2 = \frac{1}{4} + f + 8g > 0, \left(1 - f - \frac{e}{2}\right)\left(\frac{1}{4} + f + 8g\right) = \frac{1}{4}.$$

Solve the third equation,

$$f^2 + \left(\frac{e}{2} + 8g - \frac{3}{4}\right)f + 4eg + \frac{e}{8} - 8g = 0.$$

It leads to $f = \dfrac{-\left(\frac{e}{2}+8g-\frac{3}{4}Big\right)\pm\sqrt{\left(\frac{e}{2}-8g-\frac{1}{4}\right)\left(\frac{e}{2}-8g-\frac{9}{4}\right)}}{2}$, and $\left(\frac{e}{2}-8g-\frac{1}{4}\right)\left(\frac{e}{2}-8g-\frac{9}{4}\right) \geq 0$, one obtains $\frac{e}{2} - 8g \geq \frac{9}{4}$ or $\frac{e}{2} - 8g \leq \frac{1}{4}$, the Hopf bifurcation surface is

$$\begin{cases} 1 - f - \frac{e}{2} > 0 \\ \frac{1}{4} + f + 8g > 0 \\ \frac{e}{2} - 8g \leq \frac{1}{4}. \end{cases}$$

$\square$

The Hopf bifurcation of system (1) on the bifurcation surface is rather complicated. So the simple case with $e = 16g + \frac{1}{2}$, $f = \frac{1}{4} - 8g$ is considered.

Theorem 2.2. If $e = 16g + \frac{1}{2}$, $f = \frac{1}{4} - 8g$, the Jacobian matrix J has a pair of purely imaginary conjugate roots, $\lambda_{1,2} = \pm\sqrt{\frac{1}{4} + f + 8g}i$, and a negative solution $\lambda_3 = -(1 - f - \frac{e}{2})$, together with such that $\text{Re}(\lambda'_f(f_0)) \neq 0$, there for the system (1) displays a Hopf bifurcation at the point E.

P r o o f. Let $e = 16g + \frac{1}{2} = e_0$, $f = \frac{1}{4} - 8g$, the system (2) changes to

$$\dot{\tilde{x}} = \frac{1}{2}\tilde{x} - \frac{3}{2}\tilde{y} + \frac{1}{16}\tilde{z} + \left(\frac{1}{2} + 16g\right)\tilde{x}^2 + \tilde{y}\tilde{z}, \dot{\tilde{y}} = \frac{1}{2}\tilde{x} - \tilde{y} + \tilde{x}^2, \dot{\tilde{z}} = -4\tilde{x} \qquad (4)$$

and has characteristic roots $\lambda_{1,2} = \pm\frac{\sqrt{2}}{2}i$, $\lambda_3 = -\frac{1}{2}$. According to the characteristic polynomial $f(\lambda)$, it has

$$\lambda'_e = \frac{\frac{1}{2}\lambda^2}{3\lambda^2 + 2(1 - f - \frac{e}{2})\lambda + \left(\frac{1}{4} + f + 8g\right)}.$$

Substitute $\lambda_{1,2} = \pm\frac{\sqrt{2}}{2}i$, $e = e_0$ into above expression, and it obtains $\text{Re}(\lambda'_e(e_0)) = \frac{1}{6} > 0$. Consequently, the system (2) displays a Hopf bifurcation at $O(0,0,0)$, so the system (1) displays a Hopf bifurcation at E. $\square$

Next, we will use the method of projection for center manifold computation[9]. At the equilibrium $O(0,0,0)$, and under the condition of $e = 16g + \frac{1}{2} = e_0$, $f = \frac{1}{4} - 8g$, the Jacobian matrix J will be

$$J_A = \begin{pmatrix} \frac{1}{2} & -\frac{3}{2} & \frac{1}{16} \\ \frac{1}{2} & -1 & 0 \\ -4 & 0 & 0 \end{pmatrix}$$

and has characteristic roots $\lambda_{1,2} = \pm\frac{\sqrt{2}}{2}i$, $\lambda_3 = -\frac{1}{2}$ with corresponding eigenvectors

$$\xi_1 = \begin{pmatrix} -\frac{\sqrt{2}}{8}i \\ -\frac{1}{24} - \frac{\sqrt{2}}{24}i \\ 1 \end{pmatrix}, \quad \xi_2 = \begin{pmatrix} \frac{\sqrt{2}}{8}i \\ -\frac{1}{24} + \frac{\sqrt{2}}{24}i \\ 1 \end{pmatrix}, \quad \xi_3 = \begin{pmatrix} 1 \\ 1 \\ 8 \end{pmatrix}.$$

Also we can obtain the transpose matrix of J_A

$$J_B = (J_A)^{\mathrm{T}} = \begin{pmatrix} \frac{1}{2} & \frac{1}{2} & -4 \\ -\frac{3}{2} & -1 & 0 \\ \frac{1}{16} & 0 & 0 \end{pmatrix}$$

which has the same characteristic roots, and the corresponding eigenvectors are

$$\eta_1 = \begin{pmatrix} 8\sqrt{2}i \\ -8 - 8\sqrt{2}i \\ 1 \end{pmatrix}, \quad \eta_2 = \begin{pmatrix} -8\sqrt{2}i \\ -8 + 8\sqrt{2}i \\ 1 \end{pmatrix}, \quad \eta_3 = \begin{pmatrix} -8 \\ 24 \\ 1 \end{pmatrix}.$$

Let

$$q = \xi_1 = \begin{pmatrix} -\frac{\sqrt{2}}{8}i \\ -\frac{1}{24} - \frac{\sqrt{2}}{24}i \\ 1 \end{pmatrix}, \quad p = \frac{\eta_2}{\langle \eta_2, \xi_1 \rangle} = \begin{pmatrix} \frac{12\sqrt{2}i}{-4+\sqrt{2}i} \\ \frac{12-12\sqrt{2}i}{-4+\sqrt{2}i} \\ \frac{-\frac{3}{2}}{-4+\sqrt{2}i} \end{pmatrix}$$

where $\langle \alpha, \beta \rangle$ is the standard scalar product in C^n, and $\langle \alpha, \beta \rangle = \sum_{i=1}^{n} \bar{\alpha}_i \beta_i$. Obviously, q, p satisfy $J_A q = \frac{\sqrt{2}}{2} i \cdot q$, $J_B p = -\frac{\sqrt{2}}{2} i \cdot p$ and $\langle p, q \rangle = 1$, then the following computations are tedious but straightforward.

$$A(q,q) = \begin{pmatrix} -g - \frac{11}{96} - \frac{\sqrt{2}}{12}i \\ -\frac{1}{16} \\ 0 \end{pmatrix}, \quad A(q,\bar{q}) = \begin{pmatrix} g - \frac{5}{96} \\ \frac{1}{16} \\ 0 \end{pmatrix}, \quad B(q,q,\bar{q}) = 0.$$

Let $s = J_A^{-1} A(q, \bar{q})$, and $s = \begin{pmatrix} 0 \\ -\frac{1}{16} \\ 16g - \frac{7}{3} \end{pmatrix}$, then we can compute the following expressions.

$$A(q,s) = \begin{pmatrix} \frac{5}{144} - \frac{2g}{3} - \frac{2\sqrt{2}g}{3}i + \frac{7\sqrt{2}}{72}i \\ 0 \\ 0 \end{pmatrix}$$

$$t = (\sqrt{2}iE - J)^{-1} A(q,q) = \begin{pmatrix} \frac{\frac{\sqrt{2}}{72}(-19 - 96\sqrt{2}g + 96gi - 14i)}{1 + 2\sqrt{2}i} \\ \frac{-37 + 96\sqrt{2}gi + 5\sqrt{2}i}{144(1 + 2\sqrt{2}i)} \\ \frac{14 - 96g - 19\sqrt{2}i - 96\sqrt{2}gi}{18(1 + 2\sqrt{2}i)} \end{pmatrix}$$

$$A(\bar{q},t) = \begin{pmatrix} \frac{544g - 3072g^2 - 512\sqrt{2}gi - 3072\sqrt{2}g^2i - 44 + 13\sqrt{2}i}{288(1 + 2\sqrt{2}i)} \\ \frac{14 - 96g - 19\sqrt{2}i - 96\sqrt{2}gi}{144(1 + 2\sqrt{2}i)} \\ 0 \end{pmatrix}.$$

By the theory of [9], the first Lyapunov coefficient is

$$\begin{aligned} l_1(0) &= \frac{\sqrt{2}}{2}\mathrm{Re}\left(\langle p, B(q,q,\bar{q}) \rangle - 2\langle p, A(q,s) \rangle + \langle p, A(\bar{q},t) \rangle\right) \\ &= \frac{\sqrt{2}}{216}(-1536g^2 - 112g + 85) \end{aligned}$$

when $g \in \left(\frac{-7-\sqrt{2089}}{192}, \frac{-7+\sqrt{2089}}{192} \right)$, $l_1(0) > 0$ the hopf bifurcation is subcritical, when $g \in \left(-\infty, \frac{-7-\sqrt{2089}}{192} \right) \cup \left(\frac{-7+\sqrt{2089}}{192}, +\infty \right)$, $l_1(0) < 0$, the Hopf bifurcation is supercritical.

Theorem 2.3. For the Sprott E system with quadratic perturbation (1), $e = 16g + \frac{1}{2} = e_0$, $f = \frac{1}{4} - 8g$, (I) when $g \in \left(\frac{-7-\sqrt{2089}}{192}, \frac{-7+\sqrt{2089}}{192} \right)$, and $e < e_0$, the semistable limit cycle will emerge, and the Hopf bifurcation is subcritical. (II) when $g \in \left(-\infty, \frac{-7-\sqrt{2089}}{192} \right) \cup \left(\frac{-7+\sqrt{2089}}{192}, +\infty \right)$, and $e > e_0$, the stable limit cycle will emerge, and the Hopf bifurcation is supercritical.

3. DYNAMICS ANALYSIS AT INFINITY

In this section, we use the Poincare compactification method [6, 14 – 15, 17] to make a analysis of the flow of the system (1) at infinity. let $S^3 = \{r = (r_1, r_2, r_3, r_4) \in R^4 | \|r\| = 1\}$ be a Poincare unit sphere. We divide this sphere into $S_+ = \{r \in S^3, r_4 > 0\}$ (the northern hemisphere), $S_- = \{r \in S^3, r_4 < 0\}$ (the southern hemisphere) and $S^1 = \{r \in S^3, r_4 = 0\}$ (the equator). Denote the tangent hyperplanes at the point $(\pm 1, 0, 0, 0)$, $(0, \pm 1, 0, 0)$, $(0, 0, \pm 1, 0)$, $(0, 0, 0, \pm 1)$ by the local chart U_i, V_i for $i = 1, 2, 3, 4$, where $U_i = \{r \in S^3, r_i > 0\}$, $V_i = \{r \in S^3, r_i < 0\}$. Define the central projections $f^+ : R^3 \to S^3$ and $f^- : R^3 \to S^3$ by $f^{\pm}(x, y, z) = \pm \left(\frac{x}{\Delta}, \frac{y}{\Delta}, \frac{z}{\Delta}, \frac{1}{\Delta} \right)$, where $\Delta = \sqrt{1 + x^2 + y^2 + z^2}$, also define $\varphi_k : U_k \to R^3$, $\phi_k : V_k \to R^3$ by $\varphi_k = -\phi_k = \left(\frac{r_l}{r_k}, \frac{r_m}{r_k}, \frac{r_n}{r_k} \right)$ for $k = 1, 2, 3, 4$ with $1 \le l, m, n \le 4$ and $l, m, n \ne k$. We only consider the local charts U_i, V_i for $i = 1, 2, 3$ for getting the dynamics at x, y, z infinity (shown in Figure 1).
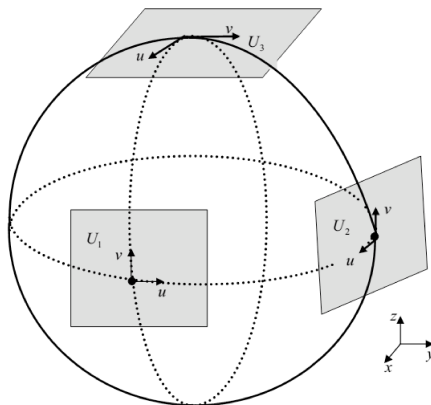
Fig. 1. Orientation of the local charts U_i, V_i for $i = 1, 2, 3$ in the positive endpoints of the x, y, z axis.

Theorem 3.1. For all values of the parameters e, f, g, the phase portrait of the system (1) on the Poincare sphere at infinity is as shown in Figure 2. There coexists a degenerate stable node and a degenerate unstable node on the $x - y$ plane. Moreover, there exists two saddle-nodes at the positive and negative of the y axis and two cusps at the positive and negative of the z axis.
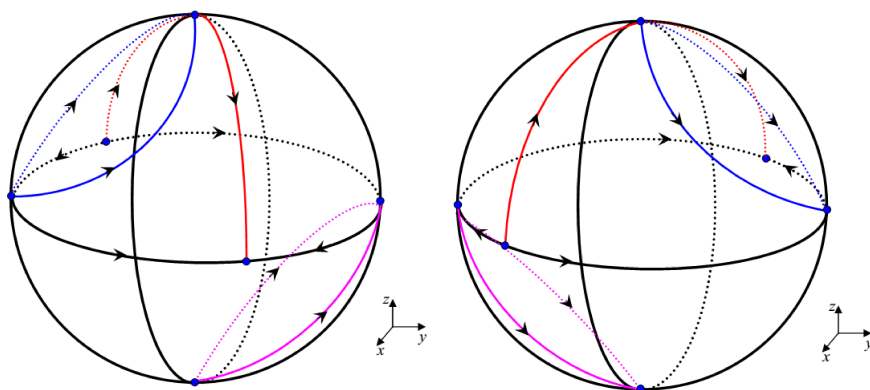
Fig. 2. The phase portraits of the system (1) on Poincare sphere:
$e > 0$ (left) and $e < 0$ (right).

In the local charts U_1 and V_1

Take the change of variables $(x, y, z) = (w^{-1}, uw^{-1}, vw^{-1})$, and $t = w\tau$, the system (1) becomes

$$\begin{aligned}
\frac{du}{d\tau} &= -u^2 v - eu - fuw - guw^2 + 1 - uw, \\
\frac{dv}{d\tau} &= -uv^2 - ev - fvw - gvw^2 + w^2 - 4w, \\
\frac{dw}{d\tau} &= -uvw - ew - fw^2 - gw^2.
\end{aligned} \tag{5}$$

If $w = 0$, the system (5) reduces to

$$\frac{du}{d\tau} - u^2 v - eu + 1, \quad \frac{dv}{d\tau} = -uv^2 - ev. \tag{6}$$

The system (6) has a unique singularity $\left(\frac{1}{e}, 0\right)$, which is a degenerate stable node for $e > 0$ and a degenerate unstable node for $e < 0$.

The flow in the local chart V_1 is the same as the flow in the local chart U_1 reversing the time, hence, the system (1) has a degenerate unstable node for $e > 0$ and a degenerate stable node for $e < 0$ on the infinite sphere. Because the system (6) is a

planar polynomial system, we can easily obtain the phase portraits of the system (6) on Poincare disc which are shown in Figure 3 in accordance with the qualitative theory of differential equations.
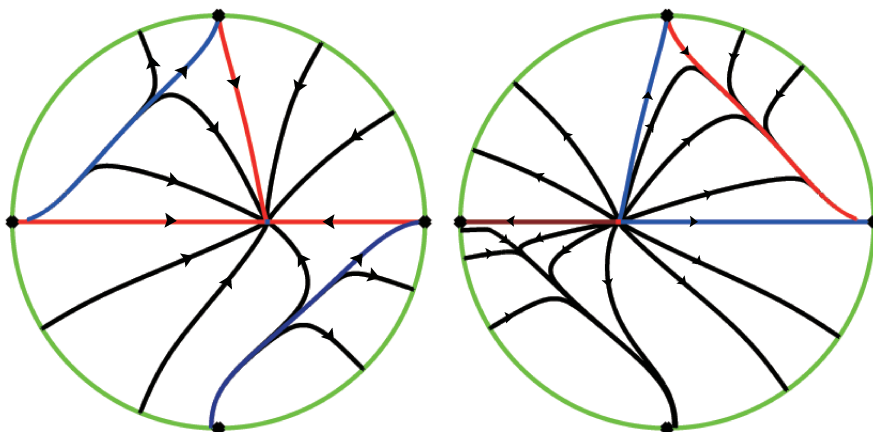
Fig. 3. The phase portraits of the system (6) on Poincare disc: $e > 0$
(left) and $e < 0$ (right).

In the local charts U_2 and V_2

Next, we study the dynamics of the system (1) at infinity of the y axis. Take the transformation $(x, y, z) = (uw^{-1}, w^{-1}, vw^{-1})$, and $t = w\tau$, the system (1) becomes

$$\frac{\mathrm{d}u}{\mathrm{d}\tau} = uw - u^3 + v + eu^2 + fwu + gw^2, \frac{\mathrm{d}v}{\mathrm{d}\tau} = -u^2v + wv + w^2 - 4uw, \frac{\mathrm{d}w}{\mathrm{d}\tau} = -u^2w + w^2. \quad (7)$$

If $w = 0$, the system (7) reduces to

$$\frac{\mathrm{d}u}{\mathrm{d}\tau} = -u^3 + v + eu^2, \frac{\mathrm{d}v}{\mathrm{d}\tau} = -u^2v. \quad (8)$$

The system (8) has a nilpotent singular point $(0,0)$ and a degenerate stable node $(e, 0)$. In accordance with Nilpotent Singular Points Theorem [7], we can know that the nilpotent singular point $(0,0)$ is a saddle-node. The flow in the local chart V_2 is the same as the flow in the local chart U_2 reversing the time. The phase portraits of the system (8) on Poincare disc are shown in Figure 4.

In the local charts U_3 and V_3

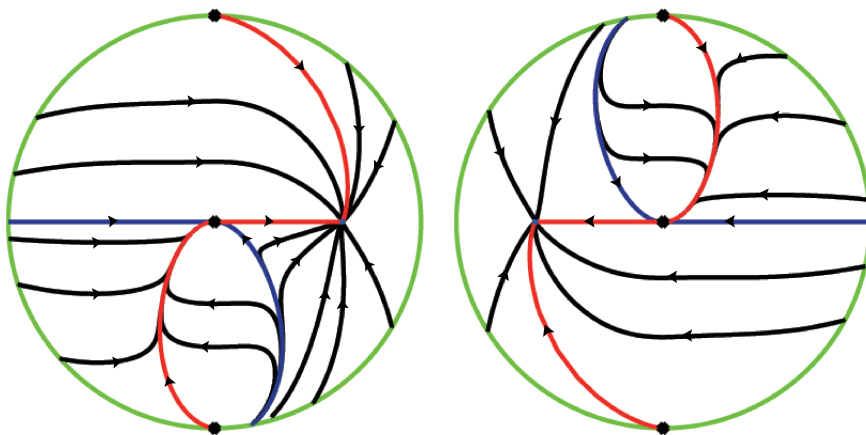Finally, we consider infinity at the z axis. Let $(x, y, z) = (uw^{-1}, vw^{-1}, w^{-1})$, and

Fig. 4. The phase portraits of the system (8) on Poincare disc: $e > 0$
(left) and $e < 0$ (right).

$t = w\tau$, the system (1) becomes

$$\frac{\mathrm{d}u}{\mathrm{d}\tau} = -uw^2 + 4wu^2 + v + eu^2 + fuw + gw^2,$$

$$\frac{\mathrm{d}v}{\mathrm{d}\tau} = -vw^2 + 4uvw + u^2 - wv, \qquad (9)$$

$$\frac{\mathrm{d}w}{\mathrm{d}\tau} = -w^3 + 4uw^2.$$

If $w = 0$, the system (9) reduces to

$$\frac{\mathrm{d}u}{\mathrm{d}\tau} = v + eu^2, \frac{\mathrm{d}v}{\mathrm{d}\tau} = u^2. \qquad (10)$$

The system (10) has only one nilpotent singular point $(0,0)$. In accordance with Nilpotent Singular Points Theorem, we can know that the nilpotent singular point $(0,0)$ is a cusp. Again the flow in the local chart V_3 is the same as the flow in the local chart U_3 reversing the time. The phase portraits of the system (10) on Poincare disc are shown in Figure 5.

From the above analysis, and taking into account its orientation as shown in Figure 1, we can get the structure of the system (1) on the sphere at infinity shown in Figure 2 (we only give the separatrix for the clarity of the figures), and verify the theorem 4. We must note that the degenerate node $\left(\frac{1}{e}, 0\right)$ of the system (6) and the degenerate node $(e, 0)$ of the system (8) are the same points in the space of xyz. From the Figure 1, we can see that in the local chart U_1, the infinity of the u axis is the origin of the u axis in the local chart U_2, so there exists a reciprocal relation from U_1 to U_2.
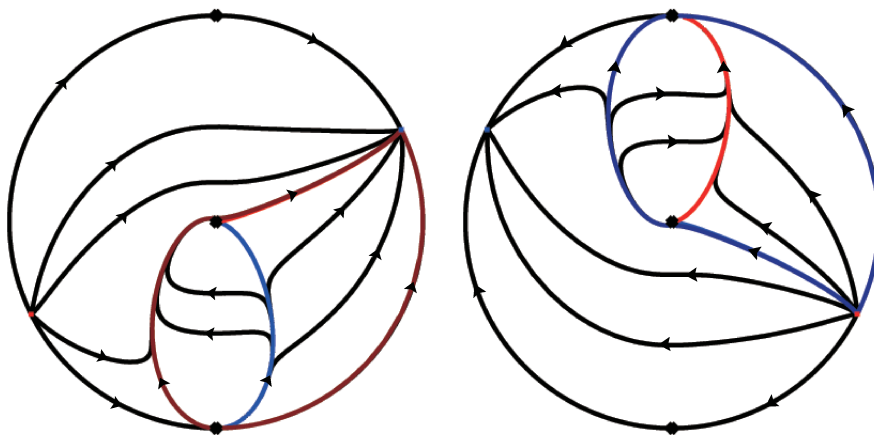
Fig. 5. The phase portraits of the system (10) on Poincare disc:
$e > 0$ (left) and $e < 0$ (right).

4. ROBUST MODIFIED FUNCTION PROJECTIVE SYNCHRONIZATION

Since the parameters of the actual system are unknown and there exists the parameters perturbation, we can rewrite the system (1) as the driven system

$$\dot{x}_1 = x_2 x_3 + e x_1^2 + f x_1 + g, \dot{x}_2 = x_1^2 - x_2, \dot{x}_3 = 1 - 4 x_1 \qquad (11)$$

and construct the response system with unknown parameters e, f, g.

$$\dot{y}_1 = y_2 y_3 + (e + \Delta e) y_1^2 + (f + \Delta f) y_1 + (g + \Delta g) + u_1, \qquad (12)$$
$$\dot{y}_2 = y_1^2 - y_2 + u_2, \quad \dot{y}_3 = 1 - 4 y_1 + u_3$$

where Δe, Δf, Δg are parameters perturbation. Let $\varepsilon_1 = y_1 - h_1(t) x_1$, $\varepsilon_2 = y_2 - h_2(t) x_2$, $\varepsilon_3 = y_3 - h_3(t) x_3$, then the error system is

$$\dot{\varepsilon}_1 = \dot{y}_1 - \dot{h}_1(t) x_1 - h_1(t) \dot{x}_1, \quad \dot{\varepsilon}_2 = \dot{y}_2 - \dot{h}_2(t) x_2 - h_2(t) \dot{x}_2, \qquad (13)$$
$$\dot{\varepsilon}_3 = \dot{y}_3 - \dot{h}_3(t) x_3 - h_3(t) \dot{x}_3$$

where $h_1(t)$, $h_2(t)$, $h_3(t)$ are modified function of projective synchronization. We also take $\hat{e}$, $\hat{f}$, $\hat{g}$ as the parameter estimates of e, f, g, and denote $\varepsilon_e = \hat{e} - e$, $\varepsilon_f = \hat{f} - f$, $\varepsilon_g = \hat{g} - g$, then the parameter error system is

$$\dot{\varepsilon}_e = \dot{\hat{e}} = -k_e \varepsilon_e, \quad \dot{\varepsilon}_f = \dot{\hat{f}} = -k_f \varepsilon_f, \quad \dot{\varepsilon}_g = \dot{\hat{g}} = -k_g \varepsilon_g. \qquad (14)$$

Theorem 4.1. When the controller u_1, u_2, u_3 satisfy $u_1 = -y_2y_3 - ey_1^2 - fy_1 - g + \dot{h}_1(t)x_1 + h_1(t)(x_2x_3 + ex_1^2 + fx_1 + g) - l\varepsilon_1 - k\frac{y_1^4\varepsilon_1 + y_1^2\varepsilon_1 + \varepsilon_1}{\sqrt{(y_1^2\varepsilon_1)^2 + (y_1\varepsilon_1)^2 + (\varepsilon_1)^2}}$, $u_2 = -y_1^2 + y_2 + \dot{h}_2(t)x_2 + h_2(t)(x_1^2 - x_2) - l\varepsilon_2$, $u_3 = -1 + 4y_1 + \dot{h}_3(t)x_3 + h_3(t)(1 - 4x_1) - l\varepsilon_3$, and $\dot{l} = \mu(\varepsilon_1^2 + \varepsilon_2^2 + \varepsilon_3^2)$, $k = \left\|(\Delta e, \Delta f, \Delta g)^{\mathrm{T}}\right\|$, then the system (11) and (12) will approach function projective synchronization.

P r o o f . Choose the Lyapunov function $V = \frac{1}{2}[\sum\limits_{i=1}^{3} \varepsilon_i^2 + \varepsilon_e^2 + \varepsilon_f^2 + \varepsilon_g^2 + \frac{1}{\mu}(l - \hat{l})^2]$, and compute the derivative of V,

$$
\begin{aligned}
\dot{V} &= \varepsilon_1[y_2y_3 + (e + \Delta e)y_1^2 + (f + \Delta f)y_1 + (g + \Delta g) + u_1 - \dot{h}_1(t)x_1 - h_1(t)\dot{x}_1] \\
&+ \varepsilon_2[y_1^2 - y_2 + u_2 - \dot{h}_2(t)x_2 - h_2(t)\dot{x}_2] + \varepsilon_3[1 - 4y_1 + u_3 - \dot{h}_3(t)x_3 - h_2(t)\dot{x}_3] \\
&+ \varepsilon_e\dot{\varepsilon}_e + \varepsilon_f\dot{\varepsilon}_f + \varepsilon_g\dot{\varepsilon}_g + \frac{1}{\mu}(l - \hat{l})\dot{l} \\
&= \varepsilon_1[\Delta ey_1^2 + \Delta fy_1 + \Delta g - \frac{k(y_1^4\varepsilon_1 + y_1^2\varepsilon_1 + \varepsilon_1)}{\sqrt{(y_1^2\varepsilon_1)^2 + (y_1\varepsilon_1)^2 + (\varepsilon_1)^2}}] \\
&- k_e\varepsilon_e^2 - k_f\varepsilon_f^2 - k_g\varepsilon_g^2 - \hat{l}(\varepsilon_1^2 + \varepsilon_2^2 + \varepsilon_3^2) \\
&= [\frac{\Delta ey_1^2\varepsilon_1 + \Delta fy_1\varepsilon_1 + \Delta g\varepsilon_1}{\sqrt{(y_1^2\varepsilon_1)^2 + (y_1\varepsilon_1)^2 + (\varepsilon_1)^2}} - k]\sqrt{(y_1^2\varepsilon_1)^2 + (y_1\varepsilon_1)^2 + (\varepsilon_1)^2} \\
&- k_e\varepsilon_e^2 - k_f\varepsilon_f^2 - k_g\varepsilon_g^2 - \hat{l}(\varepsilon_1^2 + \varepsilon_2^2 + \varepsilon_3^2) \\
&= -k\sqrt{(y_1^2\varepsilon_1)^2 + (y_1\varepsilon_1)^2 + (\varepsilon_1)^2}\left[1 - \left(\frac{(\Delta e, \Delta f, \Delta g)^{\mathrm{T}}}{k}, \frac{(y_1^2\varepsilon_1, y_1\varepsilon_1, \varepsilon_1)^{\mathrm{T}}}{\sqrt{(y_1^2\varepsilon_1)^2 + (y_1\varepsilon_1)^2 + (\varepsilon_1)^2}}\right)\right] \\
&- k_e\varepsilon_e^2 - k_f\varepsilon_f^2 - k_g\varepsilon_g^2 - \hat{l}(\varepsilon_1^2 + \varepsilon_2^2 + \varepsilon_3^2) \leq 0
\end{aligned}
$$

by the theory of stability, the error system (13) will be stable, i. e. the driven system (11) and the response system (12) will approach function projective synchronization. $\square$

5. NUMERICAL SIMULATION

Let $g = 0.02$, $f = 0.09$, then $e_0 = 0.82$, take $e = 0.2$, and the equilibrium becomes $E\left(\frac{1}{4}, \frac{1}{16}, -0.88\right)$, and the corresponding characteristic values are $\lambda_{1,2} = -0.0852 \pm 0.6194i$, $\lambda_3 = -0.6394$, obviously, the equilibrium is a stable node-foci, and the limit cycle is semistable (see Figure 6).

Let $g = 0.3$, $f = -2.15$, then $e_0 = 5.3$, take $e = 5.5$, and the equilibrium becomes $E\left(\frac{1}{4}, \frac{1}{16}, -1.7\right)$, and the corresponding characteristic values are $\lambda_{1,2} = 0.0347 \pm 0.7289i$, $\lambda_3 = -0.4694$, obviously, the equilibrium is a unstable saddle-foci, and the limit cycle is stable (see Figure 7).

To investigate the feasibility of the supposed controller in section 4, we take $g = 0.02$, $f = -0.1$, $e_0 = 0.06$ we can know that the driven system (11) is a chaotic system by Ref. [25], meanwhile, we take $k = 0.03$, $k_1 = k_2 = k_3 = 1$, $\mu = 0.1$, $\Delta e = 0.02\sin t$, $\Delta f = 0.02\cos t$, $\Delta g = -0.02\sin t$, $h_1(t) = 0.02 + 0.01\sin\frac{\pi t}{40}$, $h_2(t) = 0.03 + 0.02\sin\frac{\pi t}{40}$, $h_3(t) = 0.04 + 0.03\sin\frac{\pi t}{40}$, the chaotic attractor projection in $x - y$ plane of the driven system and response system shown in Figure 8. The synchronization of the driven system and response system shown in Figure 9, and from the Figure 10, we can see the error of the driven system and response system equals zeros. Since the parameters of the system are unknown, the estimated values of parameters e, f, g are shown in Figure 11.
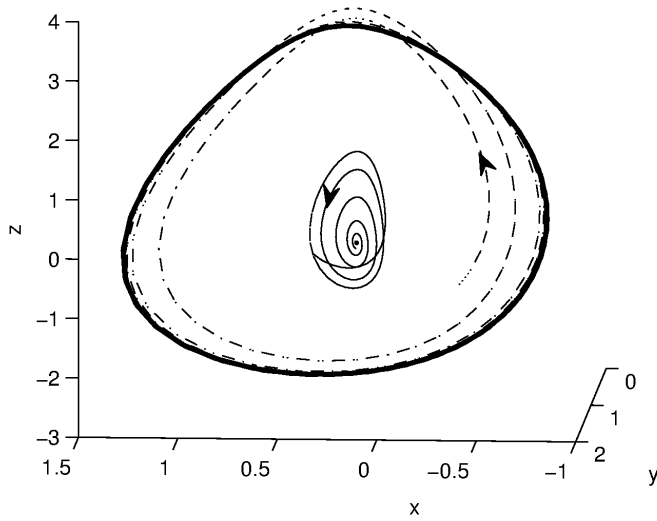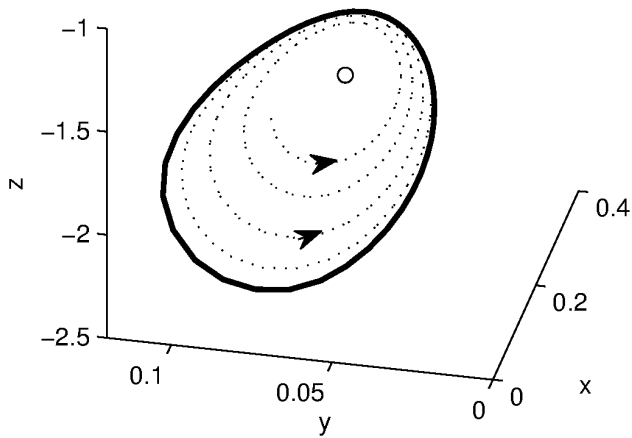
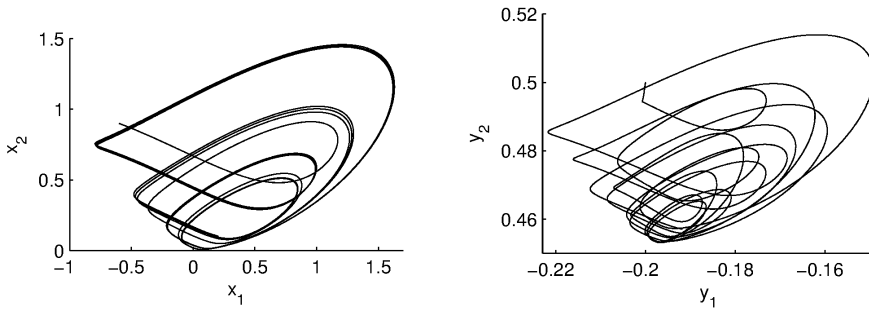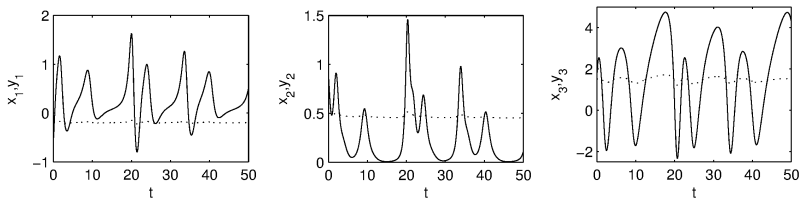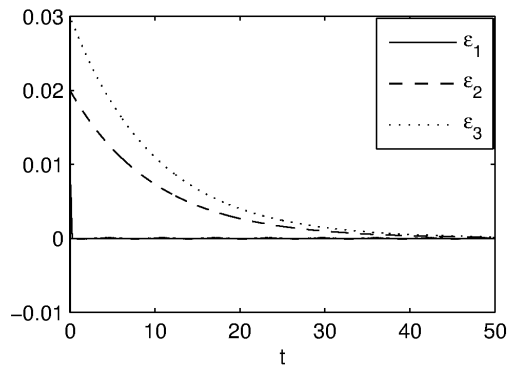**Fig. 6.** Subcritical hopf bifurcation for $g = 0.02$.

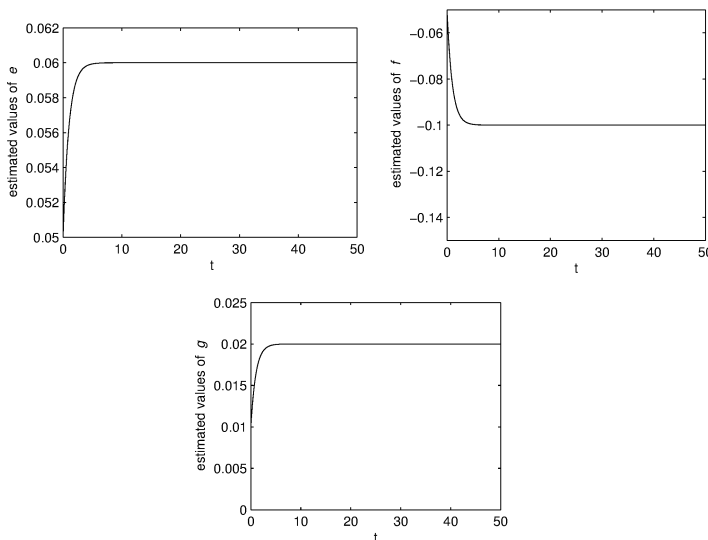**Fig. 7.** Supercritical hopf bifurcation for $g = 0.3$.

Fig. 8. Chaotic attractor projection in $x - y$ plane of the driven system and response system.

Fig. 9. Synchronization of the driven system and response system.

Fig. 10. Evolution of the error system.

Fig. 11. Evolution of parameters estimated values.

6. CONCLUSION

This paper deals with the dynamics and the synchronization of a simple chaotic system with stable equilibrium. The Hopf bifurcation of this system is computed by the method of projection for center manifold, and the subcritical and the supercritical Hopf bifurcation are obtained. Moreover, a complete description of the dynamics of this system at infinity is given using the Poincare compactification of polynomial vector in R^3. Also the RMFPS for this special chaotic system is proposed, and proved by the direct Lyapunov method. Numerical simulations confirms the correctness of the Hopf bifurcation analysis and the efficiency of the proposed synchronization strategy. Indeed, the global dynamical behaviors and the geometrical structure of this system have not been presented completely. The generation mechanism of the chaos for this special system, also with the algebra structure criteria (or normal form) for this system need to be studied. Furthermore, the chaos control and synchronization such as fractional controller for this system still need to be designed, and the corresponding fractional order chaotic system needs to be constructed and considered. These will be provided in future works.

Moreover, in future works, we will use the proposed analysis method to investigate some complex chaotic systems, such as the typical multi-scroll chaotic systems [18] by some effective design methods using trigonometric functions, cellular neural networks, nonlinear modulating functions etc and the networked chaotic systems [3−5]. It is expected that more detailed theory analysis will be provided in a forthcoming paper.

REFERENCES

[1] G. R. Chen and T. Ueta: Yet another chaotic attractor. Int. J. Bifur. Chaos *9* (1999), 1465–1466.

[2] Y. Chen, L. Cao, and M. Sun: Robust midified function projective synchronization in network with unknown parameters and mismatch parameters. Int. J. Nonlinear Sci. *10* (2010), 17–23.

[3] Y. Chen, J. H. Lü, and Z. L. Lin: Consensus of discrete-time multi-agent systems with transmission nonlinearity. Automatica *49* (2013), 1768–1775.

[4] Y. Chen, J. H. Lü, X. H. Yu, and D. J. Hill: Multi-agent systems with dynamical topologies: Consensus and applications. IEEE Circuits Syst. Magazine *13* (2013), 21–34.

[5] Y. Chen, J. H. Lü, X. H. Yu, and Z. L. Lin: Consensus of discrete-time second order multi-agent systems based on infinite products of general stochastic matrices. SIAM J. Control Optim. *51* (2013), 3274–3301.

[6] A. Cima and J. Llibre: Bounded polynomial vector field. T. Amer. Math. Soc. *318* (1990), 557–579.

[7] F. Dumortier, J. Llibre, and J. C. Artes: Qualitative Theory of Planar Differential Systems. Springer, Berlin 2006.

[8] A. P. Kuznetsov, S. P. Kuznetsov, and N. V. Stankevich: A simple autonomous quasiperiodic self-oscillator. Commun. Nonlinear Sci. Numer. Simul. *15* (2010), 1676–1681.

[9] Y. A. Kuznetsov: Elements of Applied Bifurcation Theory. Springer-Verlag, New York 1998.

[10] T. H. Lee and J. H. Park: Adaptive functional projective lag synchronization of a hyperchaotic Rössler system. Chin. Phys. Lett. *26* (2009), 090507.

[11] G. A. Leonov and N. V. Kuznetsov: Prediction of hidden oscillations existence in nonlinear dynamical systems: analytics and simulation. Adv. Intelligent Syst. Comput. *210* (2013), 5–13.

[12] G. A. Leonov, N. V. Kuznetsov, and V. I. Vagaitsev: Localization of hidden Chua's attractors. Phys. Lett. A *375* (2011), 2230–2233.

[13] H. T. Liang, Z. Wang, Z. M. Yue, and R. H. Lu: Generalized synchronization and control for incommensurate fractional unified chaotic system and applications in secure communication. Kybernetika *48* (2012), 190–205.

[14] Y. J. Liu: Analysis of global dynamics in an unusual 3D chaotic system. Nonlinear Dyn. *70* (2012), 2203–2212.

[15] Y. J. Liu and Q. G. Yang: Dynamics of the Lü system on the invariant algebraic surface and at infinity. Int. J. Bifur. Chaos *21* (2011), 2559–2582.

[16] E. N. Lorenz: Deterministic non-periodic flow. J. Atmospheric Sci. *20* (1963), 130–141.

[17] M. Messias and M. R. Gouveia: Dynamics at infinity and other global dynamical aspects of Shimizu–Morioka equations. Nonlinear Dyn. *69* (2012), 577–587.

[18] C. W. Shen, S. M. Yu, J. H. Lü, and G. R. Chen: A systematic methodology for constructing hyperchaotic systems with multiple positive Lyapunov exponents and circuit implementation. IEEE Trans. Circuits-I *61* (2014), 854–864.

[19] J. C. Sprott: Some simple chaotic flows. Phys. Rev. E *50* (1994), 647–650.

[20] K. S. Sudheer and M. Sabir: Adaptive modified function projective synchronization between hyperchaotic Lorenz system and hyperchaotic Lu system with uncertain parameters. Phys. Lett. A *373* (2009), 3743–3748.

[21] A. Vaněček and S. Čelikovský: Control systems: From Linear Analysis to Synthesis of Chaos. Prentice–Hall, London 1996.

[22] X. Wang and G. R. Chen: A chaotic system with only one stable equilibrium. Commun. Nonlinear Sci. Numer. Simul. *17* (2012). 1264–1272.

[23] Z. Wang: Existence of attractor and control of a 3D differential system. Nonlinear Dyn. *60* (2010), 369–373.

[24] Z. Wang, Y. X. Li, X. J. Xi, and L. Lü: Heteoclinic orbit and backstepping control of a 3D chaotic system. Acta Phys. Sin. *60* (2011), 010513.

[25] Z. C. Wei and Z. Wang: Chaotic behavior and modified function projective synchronization of a simple system with one stable equilibrium. Kybernetika *49* (2013), 359–374.

[26] Q. G. Yang and G. R. Chen: A chaotic system with one saddle and two stable node-foci. Int. J. Bifur. Chaos *18* (2008), 1393–1414.

Zhen Wang, 1. Department of Applied Science, Xijing University, Xi'an, 710123. P. R. China.
2. Shaanxi Key Laboratory of Complex System Control and Intelligent Information Processing, Xi'an, 710048. P. R. China.
   e-mail: williamchristian@163.com

Wei Sun, Department of Applied Science, Xijing University, Xi'an, 710123. P. R. China.
   e-mail: sunwei@xijing.edu.cn

Zhouchao Wei, Corresponding author. School of Mathematics and Physics, China University of Geosciences, Wuhan, 430074. P. R. China.
   e-mail: weizhouchao@163.com

Xiaojian Xi, Department of Applied Science, Xijing University, Xi'an, 710123. P. R. China.
   e-mail: huixiaojian@xijing.edu.cn